Hubbard model: Functional-integral approach and diagrammatic perturbation theory

Cláudio A. Macêdo
Departamento de Física, Universidade Federal de Sergipe, 49 000 Aracaju, Brazil

Maurício D. Coutinho-Filho
Departamento de Física, Universidade Federal de Pernambuco, 50 739 Recife, Brazil
(Received 22 May 1990)

We present a careful analysis of the functional-integral approach as applied to the Hubbard model in the framework of diagrammatic perturbation theory. It is demonstrated that a proper comprehension of the formalism can be attained and that the functional-integral method is a very systematic technique, free of ambiguity. In particular, additional exact relations among physical quantities of interest are derived in the context of the formalism.

I. INTRODUCTION

Functional-integral (FI) methods have been widely used to describe physical properties of quantum-mechanical many-particle systems, including correlation effects in interacting Fermi systems.[1] However, the use of these methods to treat both the Hubbard and Anderson models[2] has been hindered by many technical and conceptual difficulties.[3,4] In fact, through the years the method has been variously termed[4] "arbitrary," "ambiguous," and even "enigmatic."

In the context of itinerant-electron magnetism, the application of FI methods has been based on the use of the Hubbard-Stratonovich transformation.[5] Using this identity in the calculation of the partition function of the system, one transforms the interacting fermion problem to one involving space- and time-varying auxiliary fields (bosonization) with complicated field interactions.[6] In the literature[4] it is often pointed out that the difficulties of the method arise from the fact that it may be possible to resolve the electron interaction into quadratic forms of spin and electron number operators (properly applying the Hubbard-Stratonovich transformation) in an infinite number of ways. If the partition function is calculated exactly, the final result is obviously independent of the decomposition used. However, if different decompositions are exploited by nonrigorous approaches, one obtains distinct results and, as a consequence, an apparent ambiguity. These questions led Castellani and Di Castro[4] to conclude that a clarification of the formal apparatus in which this problem has been formulated is preliminary to any practical application to a specific physical situation. This clarification is urgent because the model has been widely used to describe very diverse physical systems such as liquid ^{3}He, low-dimensional conductors, and more recently, extended versions of it have been invoked to explain the basic mechanisms underlying the high-temperature superconducting copper oxides.

In this paper we present a careful analysis of the FI formalism as applied to the Hubbard model. This is done in the framework of diagrammatic perturbation theory.[7] We demonstrate that we can attain a proper comprehensioin of the formalism and that the FI method is a very systematic technique, free of ambiguity. Our results will help to clarify the proper application of FI methods to the Hubbard and similar model systems. Recently, a Letter concerning this subject has been published.[8]

This paper is organized as follows. In Sec. II the partition function in a generalized FI representation is introduced. This is done for a generalized transformation of the electron interaction into quadratic forms of spin and electron number operators. We then compare the several classes of representation of the formalism using a diagrammatic perturbative analysis of the thermodynamical potential. In Sec. III we calculate various basic physical quantities within the framework of a systematic diagrammatic analysis using the FI method. In particular, additional exact relations among these quantities are derived and the rules to calculate them are presented. Section IV summarizes the conclusions of our work.

II. CRITICAL ANALYSIS OF THE GENERALIZED FUNCTIONAL-INTEGRAL REPRESENTATION

We consider the single-band Hubbard model with the Hamiltonian

$$H=\sum_{i,j,\sigma}(t_{ij}-\sigma\mu_B h\delta_{i,j})c_{i\sigma}^{\dagger}c_{j\sigma}+U\sum_i n_{i\uparrow}n_{i\downarrow}\ , \qquad (1)$$

where t_{ij} is the hopping integral between sites i and j, h is an externally applied small magnetic field, U is the on-site Coulomb repulsion between electrons of different spins, $c_{i\sigma}^{\dagger}$ ($c_{i\sigma}$) are creation (annihilation) operators for an electron of spin σ, and $n_{i\sigma}$ is the electron number operator.

The functional-integral formulation of the Hubbard model requires the representation of the Coulomb interaction of (1) in terms of squares of one-body charge and spin operators. We adopt the following identity:[9]

$$n_{i\uparrow}n_{i\downarrow}=-\tfrac{1}{2}(b_c-1)n_i-\sum_{\alpha=c}^{x,y,z}b_\alpha(S_i^\alpha)^2\ , \tag{2a}$$

$$n_i=n_{i\uparrow}+n_{i\downarrow},\quad S_i^\alpha=\sum_{\sigma,\sigma'}c_{i\sigma}^\dagger S_{\sigma,\sigma'}^\alpha c_{i\sigma'}\ , \tag{2b}$$

where $S_{\sigma,\sigma'}^c=\frac{1}{2}i\delta_{\sigma,\sigma'}$, and $S_{\sigma,\sigma'}^\alpha$ with $\alpha=x,y,z$ are the spin-$\frac{1}{2}$ matrix elements. The parameters b_α satisfy the constraint $\sum_\alpha b_\alpha=2$.

Using the above equations and the Hubbard-Stratonovich transformation,[5] the grand partition function

$$Z=\mathrm{Tr}\exp\left[-\beta\left[H-\mu\sum_{i,\sigma}n_{i\sigma}\right]\right]\ , \tag{3}$$

where β is the inverse of the temperature and μ is the chemical potential, can be written in the form

$$Z=Z_0\int D\xi_q^\alpha\exp\left[-\tfrac{1}{2}\sum_{\alpha,q}\xi_q^\alpha\xi_{-q}^\alpha+\mathrm{Tr}_{\{k,\sigma\}}\ln(\mathbb{1}-\mathsf{V}\mathsf{G}^0)\right]\ , \tag{4a}$$

$$\mathsf{V}_{k,k'}^{\sigma,\sigma'}=-\left[\frac{2\beta U}{N}\right]^{1/2}\sum_\alpha(b_\alpha)^{1/2}\xi_{k-k'}^\alpha S_{\sigma,\sigma'}^\alpha\ . \tag{4b}$$

In (4a), Z_0 is the partition function of the noninteracting system and ξ_q^α are the Fourier transforms of the auxiliary fields; $q\equiv(\mathbf{q},\omega_v)$ [$k\equiv(\mathbf{k},\omega_n)$] indicate wave vectors and boson [fermion] Matsubara frequencies; N is the number of sites and G^0 is the noninteracting one-electron Green's function,

$$G_{\sigma\sigma'}^0(k,k')=G_\sigma^0(k)\delta_{k,k'}\delta_{\sigma,\sigma'}\ ,$$
$$G_\sigma^0(k)=(i\omega_n-\beta\varepsilon_{\mathbf{k}\sigma})^{-1}\ , \tag{4c}$$

$$\varepsilon_{\mathbf{k}\sigma}=\varepsilon_{\mathbf{k}}^0-\sigma\mu_B h-\mu-\frac{U}{2}(b_c-1)\ , \tag{4d}$$

where $\varepsilon_{\mathbf{k}}^0$ are the band energies.

The question remains of the necessity and physical significance of the various auxiliary fields conjugate to the spin and charge operators. Among the infinite possibilities of writing $n_{i\uparrow}n_{i\downarrow}$, two are special ones: When $b_x=b_y=0$ and $b_c+b_z=2$, we call them longitudinal decompositions because the system is expressed in terms of response to longitudinal auxiliary fields. Conversely, when $b_c=b_z=0$ and $b_x+b_y=2$, we have transverse decompositions and response to transverse auxiliary fields. The physical meaning of each representation becomes transparent when we develop a diagrammatic perturbative analysis of the thermodynamical potential

$$\Omega=-\beta^{-1}\ln Z\ , \tag{5}$$

using the free-field propagator in order to generate the same Feynman diagrams found when using the canonical operator formalism in the context of many-body theory.[10]

The following form holds for Ω when one uses the linked-cluster theorem:

$$\Omega=\Omega_0-\beta^{-1}\left\langle\exp\left[\sum_{l=1}^{\infty}X_l\right]-1\right\rangle_{0c}\ , \tag{6a}$$

where Ω_0 is the thermodynamical potential of the noninteracting system,

$$\langle\cdots\rangle_{0c}=\int D\xi_q^\alpha\cdots\exp\left[-\tfrac{1}{2}\sum_{\alpha,q}\xi_q^\alpha\xi_{-q}^\alpha\right] \tag{6b}$$

indicates connected diagrams only, and

$$x_l=-l^{-1}\mathrm{Tr}(\mathsf{V}\mathsf{G}^0)^l\ . \tag{6c}$$

Expanding the exponential function in (6a), we get a multiple power series in ξ_q^α, including averages of the type $\langle\xi_{q_1}^{\alpha_1}\xi_{q_2}^{\alpha_2}\cdots\xi_{q_n}^{\alpha_n}\rangle_{0c}$. Using the Wick theorem, a contraction defined by

$$\langle\xi_{q_1}^{\alpha_1}\xi_{q_2}^{\alpha_2}\rangle_0=\delta_{q_1,q_2}\delta_{\alpha_1,\alpha_2}\ , \tag{7}$$

we can generate all diagrams of the theory.

For longitudinal decompositions, the diagrams of order U^n are generated by terms of the type $\langle X_{l_1}X_{l_2}\cdots\rangle_{0c}$, for $l_1+l_2\cdots=2n$, because each X_l contributes with a power $U^{l/2}$. Terms with $l_1+l_2+\cdots=2n+1$ do not appear because Gaussian averages of an odd product of factors are null. The expressions of contributions to first order in U, for example, are

$$\langle X_1^2/2!\rangle_{0c}=-\frac{1}{2}\left[\frac{\beta U}{2N}\right]\sum_\sigma\left[(b_c-b_1)\left[\sum_k G_\sigma^0(k)\right]\left[\sum_{k'}G_\sigma^0(k')\right]+2\left[\sum_k G_\sigma^0(k)\right]\left[\sum_{k'}G_{-\sigma}^0(k')\right]\right] \tag{8}$$

and

$$\langle X_2\rangle_{0c}=\frac{1}{2}\left[\frac{\beta U}{2N}\right](b_c-b_1)\sum_{\sigma,q,k}G_\sigma^0(k)G_\sigma^0(k+q)\ . \tag{9}$$

In Fig. 1 we show the diagrams of (8) and (9) as well as the diagrams to order U^2 using standard rules of the canonical diagrammatic formalism.[10] In the next section, diagram rules in the context of the FI method are discussed. One should note that diagrams with coefficients depending on the parameters b_α are spurious because they are related to forbidden equal-spin electron interactions,[11] thus violating Pauli's principle. As expected, these spurious diagrams cancel out when grouped order by order in a power series of U. However, since any X_l contributes to the generation of diagrams to all orders in U, beginning with $U^{l/2}$ for l even or with $U^{(l+1)/2}$ for l odd, any approximation that truncates the expansion in (6) carries effects of spurious diagrams, unless $b_c=b_z$. Thus, among the infinite number of longitudinal decompositions, i.e.,

$$n_{i\uparrow}n_{i\downarrow}=-\tfrac{1}{2}(b_c-1)n_i-b_c(S_i^c)^2-b_z(S_i^z)^2\ \text{ with } b_c+b_z=2\ , \tag{10}$$

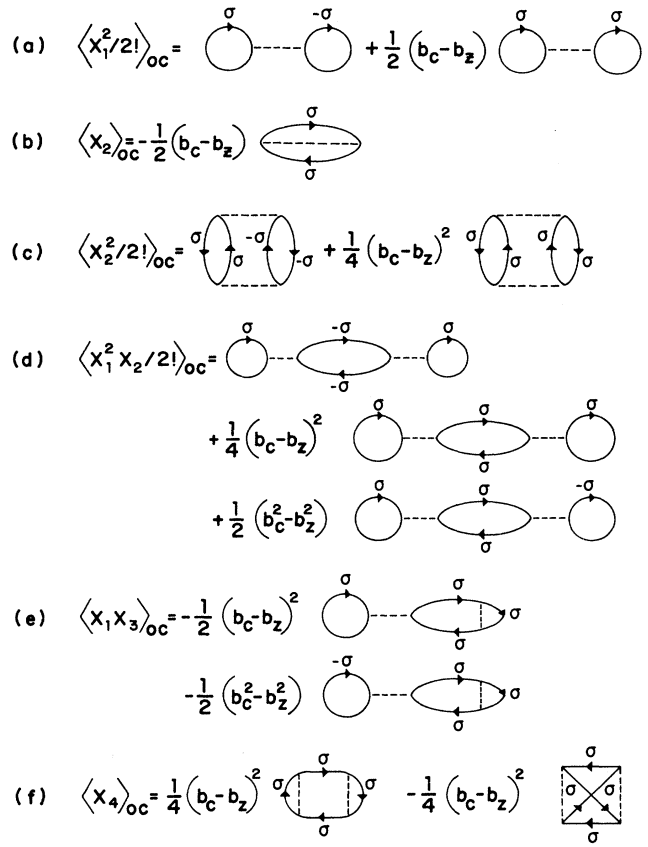

FIG. 1. Diagrams contributing to the thermodynamical potential using longitudinal decompositions. (a) and (b) Diagrams to order U. (c)–(f) Diagrams to order U^2. Solid lines represent noninteracting electron Green's function and dashed lines the interaction U. Note that the coefficients depending on b_α vanish in each order of U.

the unique decomposition free of spurious diagrams is ($b_c = b_z = 1$)

$$n_{i\uparrow} n_{i\downarrow} = -(S_i^c)^2 - (S_i^z)^2 \ . \tag{11}$$

In what follows we denote the expression (11) by the L decomposition.

To further understand this result, let us rewrite (10) in terms of electron number operators, i.e.,

$$n_{i\uparrow} n_{i\downarrow} = -\tfrac{1}{2}(b_c - 1)(n_{i\uparrow} + n_{i\downarrow}) + \tfrac{1}{4}(b_c - b_z)(n_{i\uparrow}^2 + n_{i\downarrow}^2) + \tfrac{1}{2}(b_c + b_z) n_{i\uparrow} n_{i\downarrow} \ . \tag{12}$$

Observing (12), we enlighten the origin of spurious diagrams for decompositions having $b_c \neq b_z$. Since $b_c + b_z = 2$, the first two terms in (12) must nullify. However, for that to occur in the general case $b_c \neq b_z$, one needs the use of the fermion property $n_\sigma^2 = n_\sigma$, but not in the special case $b_c = b_z = 1$. What in fact happens is that forbidden equal-spin electron interactions (of the type $U n_{i\sigma}^2$), implicitly contained in $(S_i^c)^2$ and $(S_i^z)^2$, generate spurious diagrams which do not fully cancel out in any approximate solution of the FI method because one-body terms (of the type $U n_{i\sigma}$) are treated exactly in the free part of the thermodynamical potential. We thus conclude that the fermion identity $n_\sigma^2 = n_\sigma$ is violated[11] in any approximate solution using a longitudinal decomposition in which $b_c \neq b_z$.

On the other hand, for transverse decompositions, i.e.,

$$n_{i\uparrow} n_{i\downarrow} = \tfrac{1}{2} n_i - b_X (S_i^x)^2 - b_y (S_i^y)^2 \quad \text{with } b_X + b_y = 2 \ , \tag{13}$$

the diagrams to order U^2 (see Fig. 2) are generated by $\langle X_2 \rangle_{0c}$, $\langle X_2^2/2! \rangle_{0c}$ and $\langle X_4 \rangle_{0c}$ since X_l in (6c) for l odd is null because of the fact that V is nondiagonal in spin space [cf. (6c) and (4b)]. Here diagrams of order U^n are also generated by terms type $\langle X_{l_1} X_{l_2} \cdots \rangle_{0c}$ for $l_1 + l_2 + \cdots = 2n$. In Fig. 2 the diagrams with coefficients proportional to $(b_x - b_y)$ are spurious because they arise as a result of interactions that violate spin conservation. Again, if we take approximations that truncate the expansion in (6), the spurious diagrams are not nullified unless we take $b_x = b_y$. Thus, among the transverse decompositions, the only one that does not generate spurious diagrams is

$$n_{i\uparrow} n_{i\downarrow} = \tfrac{1}{2} n_i - (S_i^x)^2 - (S_i^y)^2 \ , \tag{14}$$

which we denote the T decomposition.

Rewriting (13) in terms of raising and lowering spin operators, $S_i^+ = c_{i\uparrow}^\dagger c_{i\downarrow}$ and $S_i^- = c_{i\downarrow}^\dagger c_{i\uparrow}$, we obtain

$$n_{i\uparrow} n_{i\downarrow} = n_{i\uparrow} n_{i\downarrow} - \tfrac{1}{4}(b_x - b_y)[(S_i^+)^2 + (S_i^-)^2] \ . \tag{15}$$

It is clear that for $b_x \neq b_y$ the identity (13) is true only by using the fermion property $(S_i^\sigma)^2 = 0$, whereas for the T decomposition this is not required. These observations allow one to conclude that the origin of noncanceling spurious diagrams is, in this case, the approximate treatment of terms type $U(S_i^\sigma)^2$ when using transverse decompositions in which $b_x \neq b_y$.

As an example of problems arising when dealing with a decomposition generating spurious diagrams, we mention a study[12] in which $b_c = 1$ and $b_x = b_y = b_z = \frac{1}{3}$. The author develops inverse-degeneracy (ν) expansion trying to calculate corrections to the large degeneracy limit. However, because of the above-mentioned problems, the value

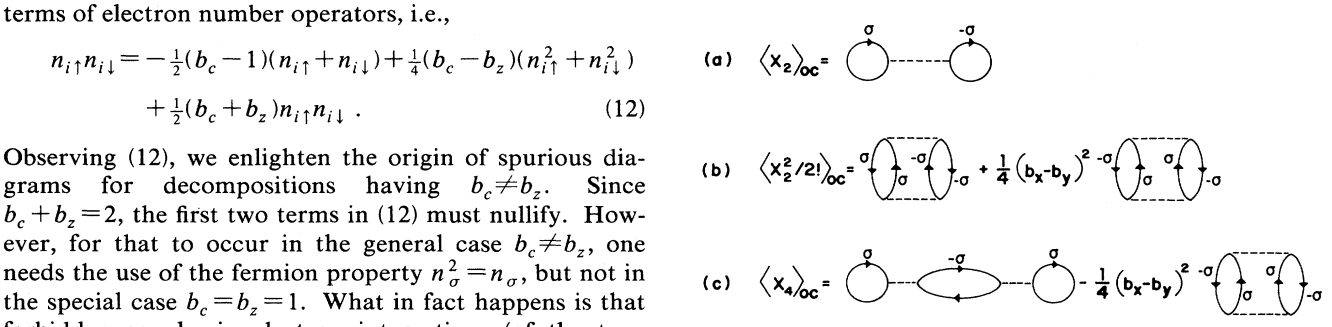

FIG. 2. Similar to Fig. 1 with use of transverse decompositions.

about which the expansion is developed in the ferromagnetic state is not the true Stoner Hartree-Fock theory of the Hubbard model. This is also manifested in the diagrams contributing to the partition function to $O(1)$ and $O(1/\nu)$ shown in Fig. 2 of Ref. 11. Three of them violate Pauli's principle and are not true corrections for the theory. The same questions can be raised for the expansion in the paramagnetic phase.[12]

Let us conclude our analysis by summarizing the main derived results.

(i) The diagrammatic series generated by decompositions in which $b_c \neq b_z$ violate Pauli's principle. Quite similarly, decompositions in which $b_x \neq b_y$ generate spurious diagrams which violate spin conservation. These spurious contributions are canceled out when grouped in a power series of U (but not in every order of the auxiliary field expansion), since any decomposition will ultimately produce the same result if a rigorous approach is used.

(ii) The L and T decompositions are the only ones to generate a diagrammatic perturbative series in which each diagram appears only once, resulting from a specific term X_l, with the right numerical coefficient found when using the canonical formalism.

(iii) Any linear combination of the L and T decompositions, i.e., using $n_{i\uparrow}n_{i\downarrow}=\alpha T+(1-\alpha)L$ (α real), is free from spurious diagrams. A given diagram may appear several times in different orders of the field expansion, but the right numerical coefficient can be found when grouping and summing up these various contributions in a power series of the physical coupling U. In particular, choosing $\alpha=\frac{1}{2}$, we obtain a decomposition in which the L and T fluctuations are treated on the same footing to any order of perturbation theory.

III. DERIVATION OF BASIC PHYSICAL QUANTITIES

The results of the preceding section suggest that we should examine the L and T decompositions in more detail. In order to derive several physical quantities of interest using the FI method, it is convenient to generalize the potential V in (4) by including sources which permit our goal. In direct space we take the following space- and imaginary-time-varying generalized potential:

$$\mathsf{W}_{i,j}^{\sigma,\sigma'}(\tau,\tau')=-\left[\left(\frac{2\beta U}{N}\right)^{1/2}\xi_1(\tau)+\beta\mathbf{h}_i(\tau)\right]\cdot\mathbf{S}_{\sigma,\sigma'}\delta_{i,j}\delta(\tau,\tau')-P_{i,j}^{\sigma,\sigma'}(\tau,\tau')\ , \tag{16}$$

where $\mathbf{h}_i(\tau)$ are proportional to local external electromagnetic fields and $P_{i,j}^{\sigma,\sigma'}(\tau,\tau')$ are nonlocal retarded potentials. The inclusion of the last potential permits the derivation of the desired physical quantities without using anticommuting (Grassmann) variables. After some manipulations we write the functional generator in the form

$$Z(\mathbf{h},P)=Z_0\int D\varphi_q^\sigma\exp\left[-\frac{1}{2}\sum_{\sigma,q}\varphi_q^\sigma\varphi_{-q}^{-\sigma}+\operatorname*{Tr}_{\{\sigma,k\}}\ln(\mathbb{1}-\mathsf{V}\mathsf{G}^0)+\operatorname*{Tr}_{\{\sigma,k\}}\ln(\mathbb{1}-\mathsf{J}\mathsf{G}\{\varphi^\sigma\})\right]\ , \tag{17}$$

where

$$\varphi_q^\sigma=\frac{1}{\sqrt{2}}(\xi_q^x+i\sigma\xi_q^y)\ , \tag{18}$$

for the T decomposition, and

$$\varphi_q^\sigma=\frac{1}{\sqrt{2}}(\xi_q^z+i\sigma\xi_q^c)\ , \tag{19}$$

for the L one; $\mathsf{G}\{\varphi_q^\sigma\}$ are the one-electron Green's functions in the presence of the auxiliary fields,

$$\mathsf{G}\{\varphi_q^\sigma\}=\mathsf{G}^0(\mathbb{1}-\mathsf{V}\mathsf{G}^0)^{-1}\ , \tag{20}$$

and J is defined by the matrix elements

$$\mathsf{J}_{k,k'}^{\sigma,\sigma'}=-\beta\mathbf{h}_{k-k'}\cdot\mathbf{S}_{\sigma,\sigma'}-P_{k,k'}^{\sigma,\sigma'}\ . \tag{21}$$

A. Thermodynamical potential

The calculation of Ω follows from (6a), but now adopting the above notation for $Z(0,0)$ in which

$$\langle\cdots\rangle_{0c}=\int D\varphi_q^\sigma\cdots\exp\left[-\tfrac{1}{2}\sum_{\sigma,q}\varphi_q^\sigma\varphi_{-q}^{-\sigma}\right] \tag{22a}$$

and

$$\langle\varphi_{q_1}^{\sigma_1}\varphi_{q_2}^{\sigma_2}\rangle_{0c}=\delta_{q_1,-q_2}\delta_{\sigma_1,-\sigma_2}\ . \tag{22b}$$

Using the T decomposition, X_l is expressed as follows:

$$X_l^{(T)}=\frac{Na^l}{\beta l}\sum_{\sigma}\sum_{q_1}\cdots\sum_{q_{l-1}}\varphi^{\sigma}_{q_1}\varphi^{-\sigma}_{q_2}\cdots\varphi^{\sigma}_{q_{l-1}}\varphi^{-\sigma}_{-(q_1+\cdots+q_{l-1})}\chi^0_{\sigma,-\sigma,\ldots,\sigma,-\sigma}(q_1,\ldots,q_{l-1}) , \tag{23a}$$

$$l=2,4,6,\ldots,a=(\beta U/N)^{1/2} , \tag{23b}$$

where

$$\chi^0_{\sigma_1,\ldots,\sigma_l}(q_1,\ldots,q_{l-1})=-\frac{\beta}{N}\sum_k G^0_{\sigma_1}(k)G^0_{\sigma_2}(k+q_1)\cdots G^0_{\sigma_l}\left[k+\sum_{i=1}^{l-1}q_i\right] \tag{24}$$

are the response of the noninteracting system to the auxiliary fields to all orders of nonlinearity.

In order to systematize the calculation of Feynmann diagrams in the FI framework using the T decomposition, one symbolizes X_l by a ring of l vertices, with wavy lines referring to auxiliary fields and solid lines specifying the noninteracting Green's function [Fig. 3(a)]. The following diagram rules for the Gaussian average of the products of rings are then obtained.

(i) The contraction (Wick theorem) of two wavy lines creates a broken line representing the interaction U in the form sketched in Fig. 3(b).

(ii) The Green's functions (solid lines) require k and σ summations satisfying conservation in the vertices.

(iii) The numeric coefficient of the diagram is given by

$$p\frac{1}{m_{l_1}!}\left[\frac{-a^{l_1}}{l_1}\right]^{m_{l_1}}\frac{1}{m_{l_2}!}\left[\frac{-a^{l_2}}{l_2}\right]^{m_{l_2}}\cdots , \tag{25}$$

where p is the number of possible ways of contracting the wavy lines, in a non-null form, and m_{l_i} is the number of rings of the type X_{l_i}.

(iv) The order in U of the diagram is given by

$$n=\tfrac{1}{2}(l_1m_{l_1}+l_2m_{l_2}+\cdots) . \tag{26}$$

For the L decomposition we obtain

$$X_l^{(L)}=\frac{Na^l}{\beta l}\sum_{\sigma}\sum_{q_1}\cdots\sum_{q_{l-1}}(-\sigma)^l\varphi^{\sigma}_{q_1}\varphi^{\sigma}_{q_2}\cdots\varphi^{\sigma}_{q_{l-1}}\varphi_{-(q_1+q_2+\cdots+q^{\sigma}_{l-1})}\chi^0_{\sigma,\ldots,\sigma}(q_1,\ldots,q_{l-1}) , \tag{27}$$

where $l=1,2,3,\ldots,$ and $\chi^0_{\sigma,\ldots,\sigma}(q_1,\ldots,q_{l-1})$ is indicated in (24). The rules for the Gaussian averages of the products of rings are similar to those described for the T decomposition with the ring represented as in Fig. 4(a). The contraction of the wavy lines as in Fig. 4(b), and the numeric coefficient (25) requires an extra factor $(-\sigma)^n$, where n is the order in U of the diagram (26).

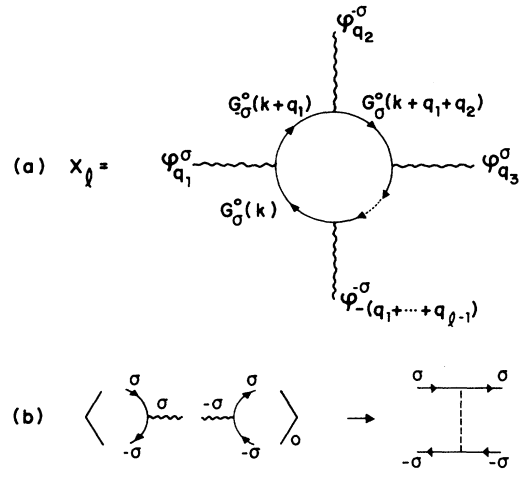

FIG. 3. (a) Functional ring for the T decomposition; (b) contraction of auxiliary transverse fields (wavy lines).

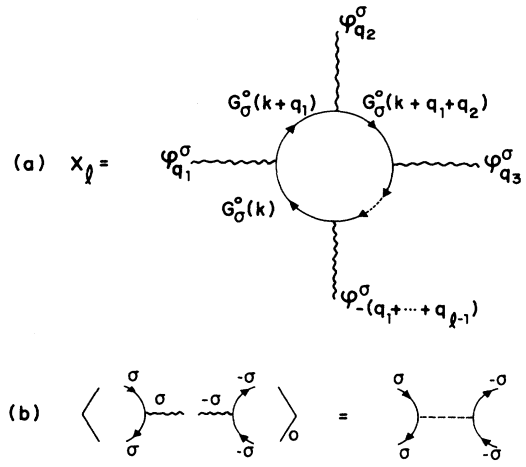

FIG. 4. (a) Functional ring for the T decomposition; (b) contraction of auxiliary longitudinal fields (wavy lines).

In the following we use the above diagram rules to study the structure of the two diagrammatic series appearing when using the T and L decompositions. This will help us to understand the characteristics of each decomposition and to elucidate several questions and doubts raised in the literature.

In the field-quadratic approximation, we obtain, using the T decomposition,

$$\Omega_{(2)}^{(T)}-\Omega_0=-\beta^{-1}\langle X_2+(X_2^2/2!)+\cdots\rangle_{0c(T)}\,, \tag{28a}$$

$$=-(1/2\beta)\sum_{\sigma,q}\{U\chi^0_{\sigma,-\sigma}(q)+\tfrac{1}{2}[U\chi^0_{\sigma,-\sigma}(q)]^2+\tfrac{1}{3}[U\chi^0_{\sigma,-\sigma}(q)]^3+\cdots\}\,, \tag{28b}$$

$$=(1/2\beta)\sum_{\sigma,q}\ln[1-U^0_{\sigma,-\sigma}(q)]\,, \tag{28c}$$

where the diagrams are indicated in Fig. 5. We see that using the T decomposition $\Omega_{(2)}^{(T)}$ gives the bare ladder diagrams of the random-phase approximation (RPA).[13] On the other hand, using the L decomposition, we have

$$\Omega_{(2)}^{(L)}-\Omega_0=-\beta^{-1}\langle X_1+(X_1^2/2!)+\cdots+X_2+X_1X_2+(X_2^2/2!)+\cdots\rangle_{0c(L)} \tag{29a}$$

$$=(NU/2\beta^2)\sum_{\sigma}[\chi^0_\sigma\chi^0_{-\sigma}-U\chi^0_{-\sigma}\chi^0_{-\sigma}\chi^0_{\sigma\sigma}(0)][1-U^2\chi^0_{\sigma\sigma}(0)\chi^0_{-\sigma,-\sigma}(0)]^{-1}$$

$$+(1/4\beta)\sum_{\sigma,q}\ln[1-U^2\chi^0_{\sigma\sigma}(q)\chi^0_{-\sigma,-\sigma}(q)]\,, \tag{29b}$$

where the diagrams are indicated in Fig. 6. Thus, using the L decomposition, we generate part of the Hartree-Fock (HF) diagrams (those in which the interaction lines can be linked by just one line) and all bare ring diagrams of the RPA,[13] showing that at this level of approximation the results are quite distinct. However, exploiting higher-order terms, we can understand the two different ways of expressing the same physical quantity Ω. Using the L decomposition, the ladder diagrams, as well as other types of diagrams, are spread out in the diagrammatic perturbative series because Ω is built up of response functions to longitudinal auxiliary fields. For example, $\langle X_3^2/2!\rangle_{0c(L)}$ generates the diagram of order U^3 of the ladder series. On the other hand, using the T decomposition, the HF and ring diagrams are spread out in the perturbative series because the systems are built up of response functions to transverse auxiliary fields. In this case, e.g., $\langle X_4\rangle_{0c(T)}$ generates the HF diagram of order U^2, whereas $\langle X_4^2/2!\rangle_{0c(T)}$ generates the diagram of order U^4 of the ring series. Therefore, both series are diagrammatically identical. It is relevant to stress that using the L decomposition all Hartree-Fock diagrams are generated by contracting the uniform components of the fields, i.e., φ_0^σ (cf. Fig. 6). This explains why in the uniform static saddle-point approximation the L decomposition is the unique choice to give the full HF result, since in this procedure this class of diagrams is taken into account to all orders of perturbation theory. On the contrary, the T decomposition generates the HF diagrams by contracting field fluctuations, i.e., φ_q^σ, giving zero contribution in the uniform static saddle-point approximation.

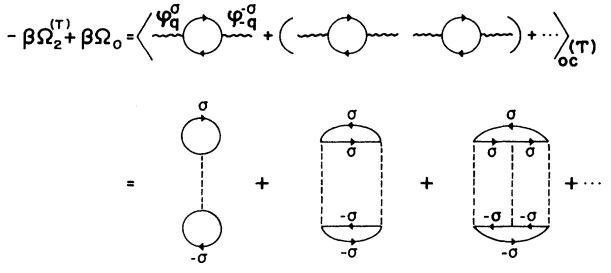

FIG. 5. Field-quadratic approximation for the thermodynamical potential with use of the T decomposition.

B. Transverse dynamic susceptibility

The transverse dynamic susceptibility can be defined by

$$\chi^{(T)}_{\sigma,-\sigma}(q)=\frac{1}{\beta N}\frac{\delta^2}{\delta h_q^\sigma\,\delta h_{-q}^{-\sigma}}\ln Z(\mathbf{h},0)\bigg|_{h=0}\,, \tag{30}$$

where

$$h_q^\sigma=\tfrac{1}{2}(h_q^x+i\sigma h_q^y)\,. \tag{31}$$

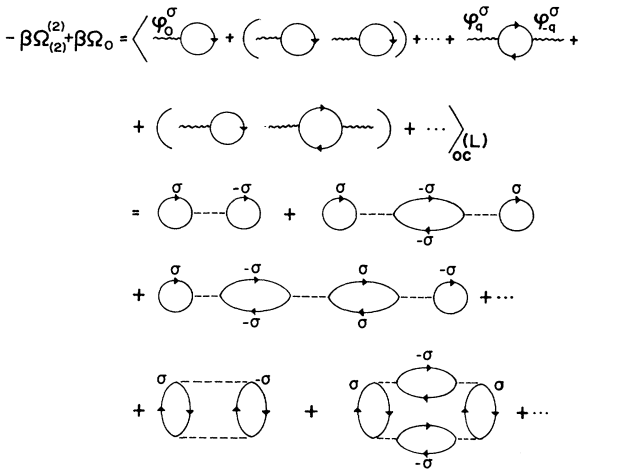

FIG. 6. Same as Fig. 5 with use of the L decomposition.

Using (17) and (18) [see also (6a)], for the T decomposition, $\chi^{(T)}$ is conveniently written in the form

$$\chi^{(T)}_{\sigma,-\sigma}(q)=U^{-1}(\langle\varphi^{\sigma}_{q}\varphi^{-\sigma}_{-q}\rangle_{(T)}-1)\ , \tag{32a}$$

$$\langle(\cdots)\rangle_{(T)}=\left\langle(\cdots)\exp\left[\sum_{l}X_{l}\right]\right\rangle_{0c}\ , \tag{32b}$$

where X_l is given by (23).

The diagrammatic study[13] of $\chi^{(T)}$ follows that developed for Ω in what concerns contractions of fields belonging to the rings as in Fig. 3 [rules (i) and (iii)]. The contraction of a single field with a field belonging to a ring generates two free propagators (solid line) as in Fig. 7; p in rule (iii) includes also the later contractions and the order in U of the diagram is now U^{n-1} [cf. rule (iv)].

In the quadratic approximation ($l=2$), we obtain the ladder approximation for $\chi^{(T)}$ (see Fig. 8):

$$\chi^{(T),(2)}_{\sigma,-\sigma}(q)=\frac{\chi^{0}_{\sigma,-\sigma}(q)}{1-U\chi^{0}_{\sigma,-\sigma}(q)}\ . \tag{33}$$

Higher-order corrections such as $U^{-1}\langle\varphi^{\sigma}_{q}\varphi^{-\sigma}_{-q}X_6\rangle_{0c}$ [Fig. 9(a)] and $U^{-1}\langle\varphi^{\sigma}_{q}\varphi^{-\sigma}_{-q}X^{2}_{4}/2!\rangle_{0c}$ [Fig. 9(b)] include self-energy corrections for the one-particle propagators and irreducible vertex corrections. Taking the corrections fully into account (see Fig. 10), $\chi^{(T)}$ satisfies a Dyson-type equation:

$$\chi^{(T)}_{\sigma,-\sigma}(q)=\Phi_{\sigma,-\sigma}(q)+\Phi_{\sigma,-\sigma}(q)U\chi^{(T)}_{\sigma,-\sigma}(q)\ , \tag{34}$$

where

$$\Phi_{\sigma,\sigma'}(q)=\sum_{k}\phi_{\sigma,\sigma'}(k,q)$$

$$=-\frac{\beta}{N}\sum_{k}\gamma_{\sigma,\sigma'}(k,k+q)G_{\sigma}(k)G_{\sigma'}(k+q)\ , \tag{35}$$

where γ denotes the irreducible vertex corrections and G_σ the one-electron Green's function including self-energy corrections.[14]

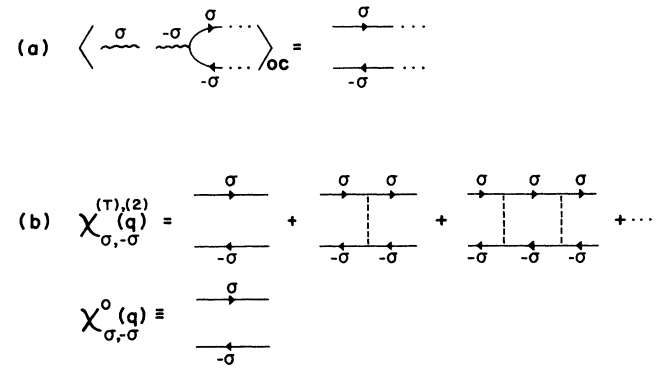

FIG. 7. (a) Contraction of a single field (wavy line) with fields bound to a ring using the T decomposition; (b) ladder approximation for the transverse susceptibility with use of the field-quadratic approximation of the T decomposition.

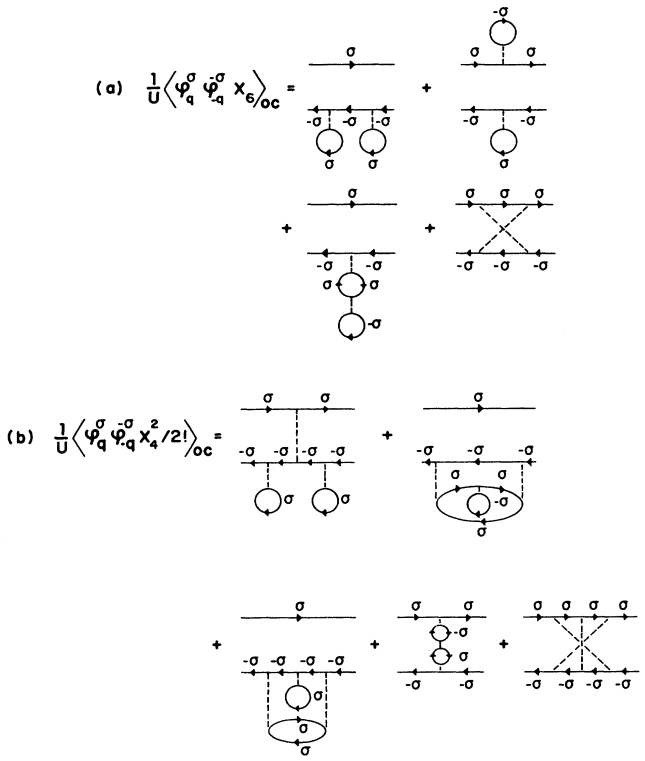

FIG. 8. Higher-order corrections to the transverse susceptibility from cumulants appearing with use of the T decomposition. They include one-particle self-energy corrections and irreducible vertex corrections.

C. Longitudinal dynamic susceptibility

The longitudinal dynamic susceptibility can be defined by

$$\chi_{zz}(q)=\tfrac{1}{4}\sum_{\sigma,\sigma'}\sigma\sigma'\chi^{(L)}_{\sigma,\sigma'}(q)\ , \tag{36a}$$

$$\chi^{(L)}_{\sigma,\sigma'}(q)=\frac{\sigma\sigma'}{\beta N}\frac{\delta^{2}}{\delta D^{\sigma}_{q}\,\delta D^{\sigma}_{q}}\ln Z(\mathbf{h},0)\Big|_{\mathbf{h}=0}\ , \tag{36b}$$

where

$$D^{\sigma}_{q}=\tfrac{1}{2}(h^{z}_{q}+i\sigma h^{c}_{q})\ . \tag{37}$$

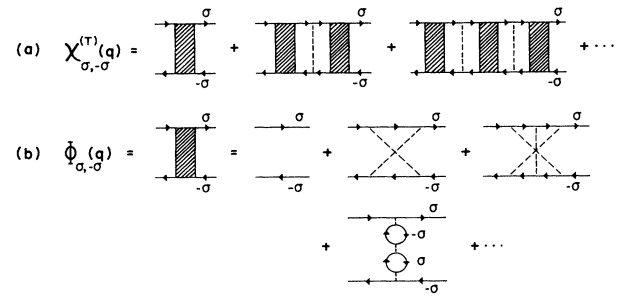

FIG. 9. (a) Diagrammatic structure of the transverse susceptibility; (b) few terms in the expansion of the irreducible "transverse" electron-hole pair propagators. (a) and (b) have been obtained with use of the T decomposition.

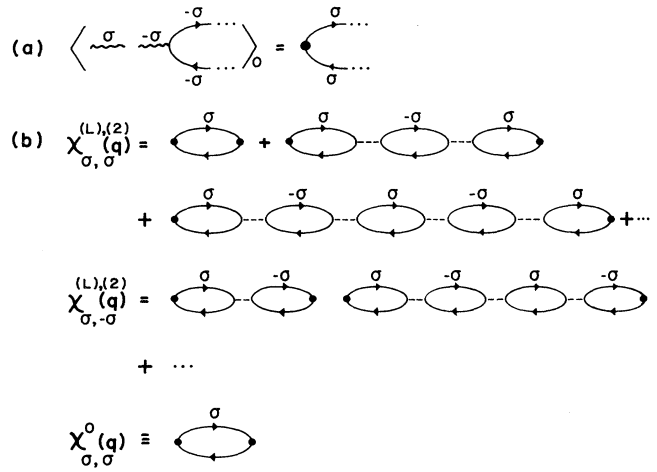

FIG. 10. (a) Same as Fig. 7 with use of the L decomposition; (b) ring approximation for the longitudinal susceptibility using the field-quadratic approximation of the L decomposition.

Using (36) and (37) [see also (6a)], for the L decomposition, $\chi^{(L)}$ is conveniently written in the form

$$\chi^{(L)}_{\sigma,\sigma'}(q)=\frac{\sigma\sigma'}{U}(\langle\varphi_q^{-\sigma}\varphi_q^{-\sigma'}\rangle_{(L)}-\delta_{\sigma,-\sigma'}) , \tag{38}$$

where $\langle\cdots\rangle_{(L)}$ is defined as in (32b) but with X_l given by (27).

The diagrammatic study $\chi^{(L)}$ is similar to the previous case, but now using the characteristics of the L decomposition, which better describe the longitudinal charge and spin fluctuations. The contraction of a single field with a field belonging to a ring generates two free propagators as in Fig. 11.

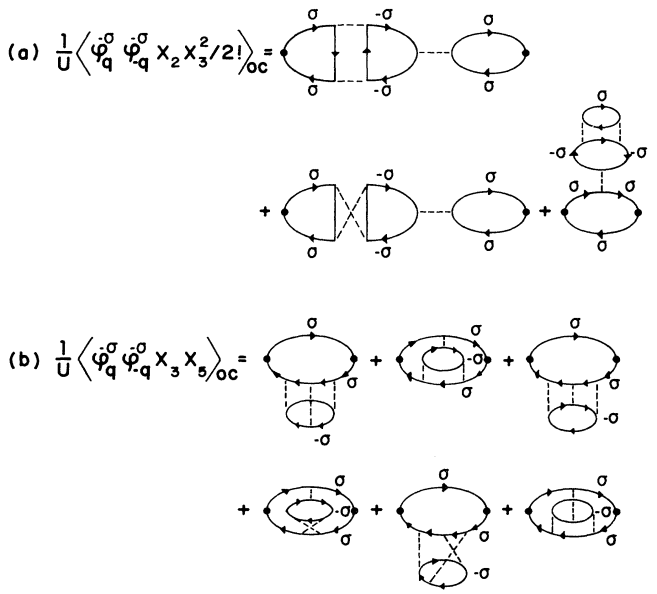

FIG. 11. (a) and (b) One-particle self-energy and irreducible vertex corrections to the longitudinal susceptibility $\chi^{(L)}_{\sigma,\sigma}$ from cummulants appearing with use of L decomposition.

In the quadratic approximation ($l=1,2$), we obtain the ring approximation for $\chi^{(L)}$ (see Fig. 12), that is.

$$\chi^{(L),(2)}_{\sigma,c}(q)=\frac{\chi^{(0)}_{\sigma,\sigma}(q)}{1-U\chi^0_{\sigma,\sigma}(q)U\chi^0_{-\sigma,-\sigma}(q)} \tag{39a}$$

and

$$\chi^{(L),(2)}_{\sigma,-\sigma}(q)=-\frac{\chi^0_{\sigma\sigma}(q)U\chi^0_{-\sigma,-\sigma}(q)}{1-U\chi^0_{\sigma,\sigma}(q)U\chi^0_{-\sigma,-\sigma}(q)} . \tag{39b}$$

Higher-order terms ($l>2$) introduce very complex self-energy and irreducible vertex corrections (cf. Fig. 12). By exploiting the diagrammatic structure of these higher-order corrections, the full susceptibility is obtained from (39) by replacing

$$\chi^0_{\sigma,\sigma}(q)=-\frac{\beta}{N}\sum_k G^0_\sigma(k)G^0_\sigma(k+q)\rightarrow\Phi_{\sigma,\sigma}(q)$$
$$=-\frac{\beta}{N}\sum_k \gamma_{\sigma,\sigma}(k,k+q)G_\sigma(k)G_\sigma(k+q) \tag{40a}$$

and

$$\chi^0_{\sigma,\sigma}(q)U\chi^0_{-\sigma,-\sigma}(q)\rightarrow\Delta_{\sigma,-\sigma}(q)$$
$$=\sum_{k,k'}\phi_{\sigma,\sigma}(k,q)\Gamma_{\sigma,-\sigma}(k,k',q)\phi_{-\sigma,-\sigma}(k',q) , \tag{40b}$$

with $\phi_{\sigma,\sigma'}(k,q)$ given by (35). We end with the following formally exact expressions:

$$\chi^{(L)}_{\sigma,\sigma}(q)=\frac{\Phi_{\sigma,\sigma}(q)}{1-U\Delta_{\sigma,-\sigma}(q)} \tag{41a}$$

and

$$\chi^{(L)}_{\sigma,-\sigma}(q)=-\frac{\Delta_{\sigma,-\sigma}(q)}{1-U\Delta_{\sigma,-\sigma}(q)} , \tag{41b}$$

with $\chi^{(L)}$ satisfying the Dyson-type equations

$$\chi^{(L)}_{\sigma,\sigma}(q)=\Phi_{\sigma,\sigma}(q)+\Delta_{\sigma,-\sigma}(q)U\chi^{(L)}_{\sigma,\sigma}(q) \tag{42a}$$

and

$$\chi^{(L)}_{\sigma,-\sigma}(q)=-\Delta_{\sigma,\sigma}(q)+\Delta_{\sigma,-\sigma}(q)U\chi^{(L)}_{\sigma,-\sigma}(q) . \tag{42b}$$

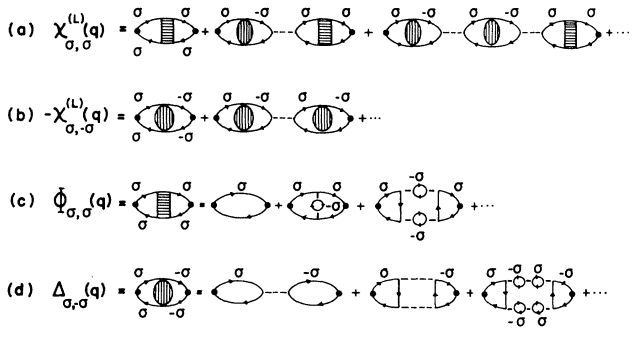

FIG. 12. (a) and (b) Diagrammatic structure of the longitudinal susceptibilities; (c) and (d) few terms in the expansion of the irreducible "longitudinal" electron-hole propagators. These results have been obtained with use of the L decomposition.

D. One-particle Green's function

The one-particle Green's function of a uniform system may be derived from

$$G_\sigma(k)=\left[\frac{\delta}{\delta P^{\sigma,\sigma}_{k,k}}\right]\ln Z(0,P)\Big|_{P=0}=\langle G^{\sigma,\sigma}_{k,k}\{\varphi^\sigma\}\rangle\ , \tag{43}$$

or from Dyson's equation for $G^{\sigma\sigma}_{k,k}\{\varphi^\sigma\}$, resulting, for both decompositions, in

$$[G^0_\sigma(k)]^{-1}G_\sigma(k)=1-a\sum_q\langle\varphi^{-\sigma}_{-q}G^{-\sigma,\sigma}_{k+q,k}\{\varphi^\sigma\}\rangle_{(T)}\ , \tag{44a}$$

$$[G^0_\sigma(k)]^{-1}G_\sigma(k)=1-a\sigma\sum_q\langle\varphi^{\sigma}_{-q}G^{\sigma,\sigma}_{k+q,k}\{\varphi^\sigma\}\rangle_{(L)}\ . \tag{44b}$$

On the other hand, the T and L susceptibilities are also obtained from the expressions

$$\chi^{(T)}_{\sigma,-\sigma}(q)=\frac{1}{2}\sum_k\left[\frac{\delta^2}{\delta P^{\sigma,\sigma}_{k,k-q}\delta h^{-\sigma}_{-q}}\right]\ln Z(\mathbf{h},P)\Big|_{\mathbf{h}=0,\,P=0} \tag{45a}$$

and

$$\chi^{(L)}_{\sigma,\sigma'}(q)=\frac{\sigma'}{N}\sum_k\left[\frac{\delta^2}{\delta P^{\sigma,\sigma}_{k,k+q}\delta D^{\sigma'}_{q}}\right]\ln Z(\mathbf{h},P)\Big|_{\mathbf{h}=0,P=0}\ , \tag{45b}$$

resulting in

$$\chi^{(T)}_{\sigma,-\sigma}(q)=\frac{\beta}{Na}\sum_k\langle\varphi^{-\sigma}_{-q}G^{-\sigma,\sigma}_{k+q,k}\{\varphi^\sigma\}\rangle_{(T)} \tag{46a}$$

and

$$\chi^{(L)}_{\sigma,\sigma'}(q)=\frac{\sigma'\beta}{Na}\sum_k[\langle\varphi^{-\sigma'}_{-q}G^{\sigma,\sigma}_{k+q,k}\{\varphi^\sigma\}\rangle_{(L)}-\delta_{q,0}\sigma' aN\bar{n}_{\sigma'}G_\sigma(k)]\ , \tag{46b}$$

where $\sigma aN\bar{n}_\sigma=\langle\varphi^{-\sigma}_0\rangle_{(L)}$. Now, using Eqs. (34), (35), and (46a), we have

$$\langle\varphi^{-\sigma}_{-q}G^{-\sigma,\sigma}_{k+q,k}\{\varphi^\sigma\}\rangle_{(T)}=-a[1+U\chi^{(T)}_{\sigma,-\sigma}(q)]\gamma_{\sigma,-\sigma}(k,k+q)G_{-\sigma}(k+q)G_\sigma(k)\ . \tag{47}$$

Substituting this result in Eq. (44a), we obtain an exact expression for the proper self-energy, defined by

$$\Sigma_\sigma(k)=[G^0_\sigma(k)]^{-1}-[G_\sigma(k)]^{-1}\ , \tag{48}$$

which for null field ($h=0$) is written as

$$\Sigma_\sigma(k)=\frac{\beta U}{N}\sum_q[1+U\chi^{(T)}_{\sigma,-\sigma}(q)]\gamma_{\sigma,-\sigma}(k,k+q)G_{-\sigma}(k+q)\ . \tag{49}$$

In the ordered phase of itinerant-electron magnets, Eq. (49) corresponds to building up the problem in terms of electron-magnon interactions,[15] the magnons being the poles of $\chi^{(T)}$. It is important to emphasize that in the context of the FI formalism this is naturally obtained through the use of the T decomposition. We also should mention that, neglecting $U\chi^{(T)}$ and vertex corrections ($\gamma=1$) in (49), we obtain the self-consistent equations of the HF approximation. Moreover, using the HF approximation for $G_{-\sigma}$ and $\gamma=1$, we get the RPA expression (33) for $\chi^{(T)}$ and the transverse contribution of the RPA for Σ_σ. Using now Eqs. (42a) and (46b), we have

$$\sigma\langle\varphi^{\sigma}_{-q}G^{\sigma}_{k+q,k}\{\varphi^\sigma\}\rangle_{(L)}=-\left[a[1-U\chi^{(L)}_{\sigma,-\sigma}(q)]\gamma_{\sigma,\sigma}(k,k+q)G_\sigma(k+q)\sum_{k'}\Gamma_{\sigma,-\sigma}(k,k',q)\phi_{-\sigma,-\sigma}(k',q)+\delta_{q,0}aN\bar{n}_{-\sigma}\right]G_\sigma(k)\ . \tag{50}$$

Finally, substituting this expression in (44b), we obtain the exact relation ($h=0$)

$$\Sigma_\sigma(k)=\beta Un_{-\sigma}+\frac{\beta U}{N}\sum_q\left[[1-U\chi^{(L)}_{\sigma,-\sigma}(q)]\gamma_{\sigma,\sigma}(k,k+q)G_\sigma(k+q)\sum_{k'}\Gamma_{\sigma,-\sigma}(k,k',q)\phi_{-\sigma,-\sigma}(k',q)\right]\ . \tag{51}$$

This is a result derived using the L decomposition and corresponds to working the problem in terms of longitudinal fluctuations. It is certainly of interest when studying charge and longitudinal spin correlations in Fermi systems. In this case, neglecting the second term on the right-hand side of (51), we obtain the HF result. In addition, taking the HF approximation for $G_{-\sigma}$ and neglecting vertex corrections ($\gamma=1$ and $\Gamma=U$), we get the RPA expression (39b) for $\chi^{(L)}$ and the longitudinal contribution of the RPA for Σ_σ.

IV. CONCLUSIONS

The above-derived results evidence that, using the FI method to describe[3] the Hubbard model [Eqs. (1)–(4)], we

may distinguish two basic or fundamental auxiliary field fluctuations: longitudinal and transverse fluctuations. The latter are associated to transverse spin fluctuations, whereas the former to both charge and longitudinal spin fluctuations. These features appear naturally incorporated in the formalism, as clearly demonstrated in the derivation of Eqs. (49) and (51). Although any formulation can be used to calculate a desired physical quantity, the convenience of the $T(L)$ decomposition is dictated by the relevance of the $T(L)$ fluctuations on the quantity of interest, as explicitly shown in the derivation of the diagrammatic structure of the $T(L)$ susceptibility. The FI formalism has the advantage of considering the $T(L)$ fluctuations in increasing order of nonlinearity [see Eqs. (23a) and (27)]. It should be observed that the results also evidence that if use is made of decompositions in which terms violating Pauli's principle or spin conservation are present, care must be exercised; otherwise, a nonrigorous approach may lead to illogical results.

Finally, we comment on the calculation of the critical properties of the system. In this case the partition function is most conveniently renormalized[16] using the decomposition in which the T and L fluctuations are taken into account on the same footing. It is then possible to show that the spin fluctuations are critically coupled together, whereas the charge fluctuations act as a background on noncritical fluctuations. This is the subject of a forthcoming paper.

ACKNOWLEDGMENTS

This work was partially supported by Conselho Nacional de Desenvolvimento Científico e Tecnológico, Coordenção de Aperfeiçoamento de Pessoal do Ensino Superior, and Financiadora de Estudos e Projetos (Brazilian Government Agencies).

[1]See, e.g., *Path Integrals and their Applications in Quantum, Statistical and Solid State Physics,* edited by G. J. Papadopoulos and J. T. DeVreese (Plenum, New York, 1978).

[2]J. Hubbard, Proc. R. Soc. London Ser. A **276**, 238 (1963); P. W. Anderson, Phys. Rev. **124**, 41 (1961).

[3]See, e.g., C. A. Macedo, M. D. Coutinho-Filho, and M. A. de Moura, Phys. Rev. B **25**, 5965 (1982), and references therein. See also papers by J. Hubbard and R. E. Prange, in *Electron Correlation and Magnetism in Narrow-Band Systems,* edited by T. Moriya (Springer, Berlin, 1981), pp. 29 and 69, respectively.

[4]R. F. Hassing and D. M. Esterling, Phys. Rev. B **7**, 432 (1973); A. A. Gomes and P. Lederer, J. Phys. (Paris) **38**, 231 (1977); C. Castellani and C. Di Castro, Phys. Lett. **70A**, 37 (1979); J. Hubbard, Phys. Rev. B **19**, 2626 (1979); **20**, 4584 (1979); R. E. Prange and V. Koreman, *ibid.* **19**, 4691 (1979); **19**, 4698 (1979).

[5]R. L. Stratonovich, Dokl. Acad. Nauk SSSR **115**, 1097 (1958) [Sov. Phys. Dokl. **2**, 416 (1958)]; J. Hubbard, Phys. Rev. Lett. **3**, 77 (1959).

[6]See, e.g., S. Q. Wang, W. E. Evenson, and J. R. Schrieffer, Phys. Rev. Lett. **23**, 92 (1969); D. R. Hamann, *ibid.* **23**, 95 (1969); R. Hamann and J. R. Schrieffer, in *Magnetism,* edited by G. T. Rado and H. Suhl (Academic, New York, 1973), Vol. 5.

[7]Alternative formulations are found in J. E. Hirsh, Phys. Rev. B **28**, 4059 (1983); **34**, 3216 (1986); G. Kotliar and A. E. Ruckenstein, Phys. Rev. Lett. **57**, 1362 (1986); R. T. Scalettar, D. J. Scalapino, R. T. Sugar, and D. Toussaint, Phys. Rev. **36**, 8632 (1987). See also U. Wolf, Nucl. Phys. **B225** [FS9], 391 (1983).

[8]C. A. Macêdo and M. D. Coutinho-Filho, Europhys. Lett. **3**, 387 (1987).

[9]The charge and spin operators used here suffice to describe itinerant-electron magnetism. If, however, one also wants to study possible superconducting phases, it may be convenient to enlarge the class of charge operators as first suggested by C. Castellani, C. Di Castro, D. Feinberg, and J. Ranninger, Phys. Rev. Lett. **43**, 1957 (1979). For a recent discussion, see R. Schumann and E. Heiner, Phys. Lett. A **134**, 202 (1988).

[10]A. L. Fetter and J. D. Walecka, in *Quantum Theory of Many-Particle Systems* (McGraw-Hill, New York, 1971).

[11]Studies along these lines have been carried out by H. Keiter, Phys. Rev. B **2**, 3777 (1970); D. Sherrington, J. Phys. C **4**, 401 (1971). Diagrammatic series using dressed propagator have been exploited by J. A. Hertz and M. A. Klenin, Phys. Rev. B **10**, 1084 (1974); S. G. Mishra and T. V. Ramakrishnan, *ibid.* **18**, 2308 (1978).

[12]J. H. Samson, Phys. Rev. B **30**, 1437 (1984).

[13]M. T. Béal-Monod, S.-k. Ma, and D. R. Fredkin, Phys. Rev. Lett. **20**, 929 (1968); W. F. Brinkman and S. Engelsberg, Phys. Rev. **169**, 417 (1968).

[14]Several aspects of the diagrammatic structure of these susceptibilities have been studied in the canonical formalism by S.-k. Ma, M. T. Béal-Monod, and D. R. Fredkin, Phys. Rev. **174**, 227 (1968); J. A. Hertz, Int. J. Magn. **1**, 253 (1971); J. A. Hertz and D. M. Edwards, J. Phys. F **3**, 2174 (1973); A. Kawabata, *ibid.* **4**, 1477 (1974); D. R. Grempel, Phys. Rev. B **27**, 4281 (1983); M. T. Béal-Monod, *ibid.* **32**, 5966 (1985).

[15]J. A. Hertz and D. M. Edwards (Ref. 14); M. Corrias, J. Phys. F **5**, L-31 (1975); S. Seki, Prog. Theor. Phys. **62**, 297 (1979); E. Kolley and W. Kolley, Phys. Status Solidi B **105**, K85 (1981); J. P. Whitehead, H. Matsumoto, and H. Umezawa, Phys. Rev. B **29**, 423 (1984), and references therein.

[16]A. A. Gomes and P. Lederer (Ref. 4); C. M. Chaves, P. Lederer, and A. A. Gomes, J. Phys. C **10**, 3367 (1977); M. D. Coutinho-Filho, J. Phys. (Paris) Colloq. **8**, C-1267 (1988); M. D. Coutinho-Filho, M. L. Lyra, and A. Nemirovsky, Solid State Commun. **74**, 1175 (1990).